Commagene Journal of Biology

Tuğrul et al., (2026) *Comm. J. Biol.* 12, 1-11.
DOI: 10.31594/commagene.1839245

e-ISSN 2602-456X

Research Article/Araştırma Makalesi

Effects of Combined *Artemisia absinthium* and Temozolomide Treatment on Apoptosis, Autophagy, and Nitric Oxide Synthase in Glioblastoma

Berrin TUĞRUL*[1], Fatih ÇÖLLÜ[2], Beyhan GÜRCÜ[3]

[1]*Manisa Celal Bayar University, Faculty of Engineering and Natural Sciences, Department of Biology, Division of Molecular Biology, Manisa, TÜRKIYE*
[2]*Manisa Celal Bayar University, Institute of Graduate Studies, Division of Biology, Manisa, TÜRKIYE*
[3]*Manisa Celal Bayar University, Faculty of Engineering and Natural Sciences, Department of Biology, Division of Zoology, Manisa, TÜRKIYE*

ORCID ID: Berrin TUĞRUL: https://orcid.org/0000-0003-0844-7766; Fatih ÇÖLLÜ: https://orcid.org/0000-0001-6978-8404; Beyhan GÜRCÜ: https://orcid.org/0000-0001-7667-7155

Received: 09.12.2025 **Revised:** 22.01.2026 **Accepted:** 29.01.2026 **Published:** 13.02.2026

Abstract: *Artemisia absinthium* (wormwood; WO) is a plant known for its anticancer potential and this study comprehensively evaluates the effects of WO, alone and in combination with Temozolomide (TMZ), on cytotoxicity, apoptosis, autophagy, mitochondrial membrane potential, cell migration, and nitric oxide synthase (NOS) responses in T98-G glioblastoma cells. Cytotoxicity, apoptosis, autophagy, mitochondrial membrane potential, and cell migration were assessed using MTT, Annexin V-FITC/PI, JC-1, monodansylcadaverine (MDC) staining, and wound healing assay, respectively. Protein levels of eNOS, iNOS, and LC3-II were examined using immunofluorescence and western blotting. WO significantly reduced T98-G cell viability in a dose- and time-dependent manner with pronounced cytotoxicity observed at 48 and 72 hours. The combined treatment increased early (24.6%) and late (40.5%) apoptosis, reducing cell viability to 31.9%. Combined treatment markedly increased autophagic vacuoles, enhancing perinuclear and cytoplasmic accumulation compared with single agents. Combined WO and TMZ treatment disrupted mitochondrial membrane potential more prominently than either agent alone, suggesting that apoptosis is mediated via the mitochondrial pathway. WO strongly inhibited T98-G cell migration, whereas TMZ and the combination had moderate suppressive effects. In T98-G cells, WO IC_{50} significantly increased eNOS ($p<0.0001$), iNOS ($p<0.0001$), and LC3 ($p<0.01$), while TMZ IC_{50} moderately increased iNOS ($p<0.05$) and combined treatment maximally elevated iNOS and LC3 ($p<0.0001$) without further affecting eNOS. Preliminary Western blot analyses qualitatively corroborated the immunofluorescence data, indicating consistent treatment-dependent trends in eNOS, iNOS, and LC3-II expression. These findings highlight the potential of WO in enhancing TMZ efficacy and provide a basis for further investigation in glioblastoma therapy.

Keywords: T98-G cell line, programmed cell death, mitochondrial dysfunction, cell migration.

Glioblastomada *Artemisia absinthium* ve Temozolomidin Kombine Uygulamasının Apoptoz, Otofaji ve Nitrik Oksit Sentaz Üzerine Etkileri

Öz: *Artemisia absinthium* (pelin otu; WO), antikanser potansiyeli ile bilinen bir bitkidir; bu çalışma, WO'nun tek başına ve Temozolomid (TMZ) ile birlikte uygulanmasının T98-G glioblastoma hücrelerinde sitotoksisite, apoptoz, otofaji, mitokondriyal membran potansiyeli, hücre göçü ve nitrik oksit sentaz (NOS) yanıtları üzerindeki etkilerini kapsamlı bir şekilde değerlendirmektedir. Çalışma esnasında sitotoksisite, apoptoz, otofaji, mitokondriyal membran potansiyeli ve hücre göçü sırasıyla MTT, Annexin V-FITC/PI, JC-1, monodansilkadaverin (MDC) boyaması ve yara iyileşme testi kullanılarak analiz edilmiştir. eNOS, iNOS ve LC3-II protein düzeyleri immünfloresan ve western blot yöntemleri kullanılarak incelenmiştir. WO, T98-G hücre canlılığını doz- ve zamana bağlı olarak anlamlı şekilde azaltmış, özellikle 48 ve 72 saatlerde belirgin sitotoksisite gözlenmiştir. Kombine tedavi erken (%24.6) ve geç (%40.5) apoptozu artırmış ve hücre canlılığını %31.9'a düşürmüştür. Kombinasyon tedavisi, tek ajanlarla karşılaştırıldığında çekirdek çevresi ve sitoplazmik birikimi artırarak otofajik vakuolleri belirgin şekilde yükseltmiştir. WO ve TMZ kombinasyonu, mitokondriyal membran potansiyelini sinerjistik biçimde bozarak apoptozun mitokondriyal yolak üzerinden gerçekleştiğini düşündürmüştür. WO, T98-G hücre göçünü güçlü biçimde inhibe ederken, TMZ ve kombinasyon tedavisinin baskılayıcı etkileri orta düzeyde kalmıştır. T98-G hücrelerinde WO IC_{50}, eNOS ($p<0.0001$), iNOS ($p<0.0001$) ve LC3 ($p<0.01$) düzeylerini anlamlı şekilde artırırken; TMZ IC_{50} iNOS düzeyini orta derecede yükseltmiştir ($p<0.05$). Kombine tedavi, eNOS üzerinde ek bir etki göstermeksizin iNOS ve LC3 düzeylerini maksimum düzeye çıkarmıştır ($p<0.0001$). Ön değerlendirme niteliğindeki Western blot analizleri, immünfloresans bulgularını niteliksel olarak destekleyerek eNOS, iNOS ve LC3 ifadelerinin tedaviye bağlı tutarlı değişim gösterdiğini ortaya koymuştur. Bu bulgular, WO'nun TMZ etkinliğini artırma potansiyelini vurgulamakta ve glioblastoma tedavisinde ileri araştırmalar için temel oluşturmaktadır.

Anahtar kelimeler: T98-G hücre hattı, programlanmış hücre ölümü, mitokondriyal disfonksiyon, hücre göçü.

1. Introduction

Glioblastoma multiforme (GBM) represents the most aggressive form of primary brain tumors originating from glial cells or their progenitors and is classified as a grade IV astrocytoma by the World Health Organization. GBM accounts for a considerable portion of malignant tumors of the central nervous system (CNS) and is defined by rapid

Corresponding author: berrin.tugrul@yahoo.com

cellular proliferation, extensive vascularization, and pronounced resistance to conventional therapies including radiotherapy and chemotherapy. Despite surgical resection and multimodal regimens involving temozolomide (TMZ), the median survival time of patients is only 12–15 months and the 5-year survival rate remains below 5% (Batash et al., 2017; Kashyap et al., 2021).

Temozolomide remains the only chemotherapeutic agent officially approved for glioblastoma treatment. It is an alkylating drug capable of crossing the blood-brain barrier (BBB) and inducing DNA methylation-driven cytotoxicity. Yet, genetic and epigenetic changes that impair processes such as apoptosis, cell cycle control, and cellular migration frequently lead to therapeutic resistance. As a result, the development of new agents that can overcome these barriers and effectively target resistant glioblastoma cells is of critical importance (Pfeffer & Singh, 2018).

Natural products have attracted considerable interest in oncology due to their chemical diversity, potent bioactivities, and relatively low toxicity profiles. Flavonoids, phenolic acids, and terpenoids, among other classes, have shown antitumor effects in multiple cancer models. Notably, *Artemisia absinthium* (*A. absinthium;* wormwood; WO) has gained attention as a potential therapeutic agent owing to its wide-ranging biological properties including antioxidant, anti-inflammatory, antiparasitic, and anticancer activities (Bora & Sharma, 2010; Dehelean et al., 2021)

Artemisia absinthium, a perennial herb of the Asteraceae family, is widely found in Europe, Asia, and North Africa. It is rich in bioactive secondary metabolites including flavonoids, coumarins, phenolic acids, sterols, and acetylenic compounds. Research indicates that *A. absinthium* extracts exert marked cytotoxic effects against various cancer cell lines, such as breast cancer (MCF-7, MDA-MB-231) and cervical cancer (HeLa), mainly via reactive oxygen species (ROS) generation and mitochondrial damage (Caner et al., 2008; Ramazani et al., 2010). Moreover, derivatives like artemisinin and artesunate have displayed significant antitumor activities in both *in vitro* and *in vivo* studies, highlighting their therapeutic potential in oncology (Mahmoudi et al., 2009; Batiha et al., 2020).

Artemisia absinthium extract and its derivatives influence apoptotic pathways by modulating the expression of key regulators such as Bcl-2 and Bax, activating caspases, and enhancing mitochondrial membrane permeability. Additionally, nitric oxide (NO) signaling contributes to its anticancer effects by promoting oxidative stress, DNA damage, and caspase activation, thereby sensitizing tumor cells to therapeutic agents (Parpura et al., 2012; Park & Lee, 2022). Although current findings indicate that *A. absinthium* can exert antitumor effects through mechanisms such as ROS-dependent apoptosis, mitochondrial dysfunction, and cell-cycle arrest, data regarding its impact in the context of GBM remain extremely limited. Therefore, an integrative approach encompassing mitochondrial dynamics, ROS generation, NO signaling, and apoptotic pathways represents an unexplored research avenue with potential relevance for GBM therapy (Wei et al., 2019).

Accordingly, this study aims to investigate the cytotoxic, apoptotic, and anti-migratory effects of WO, alone and in combination with TMZ, on the T98-G glioblastoma cell line, with particular emphasis on mitochondrial membrane potential, nitric oxide synthase (NOS) signaling, and autophagy pathways.

2. Material and Method

2.1. Cell Culture

The human glioblastoma cell line T98-G (ATCC® CRL-1690™) was cultured in DMEM (Biological Industries, 01-025-1A) supplemented with 10% fetal bovine serum (FBS; Biological Industries, 04-007-1B), 1% GlutaMax™ (Thermo Fisher, 35050061), and 1% penicillin-streptomycin (Biological Industries, 03-031-1C) at 37°C in a humidified atmosphere of 5% CO_2.

2.2. Preparation of WO Extract Stock Solution and Vehicle Control

WO was initially prepared as a methanolic total extract; the methanol was completely evaporated, and the dried residue was reconstituted in DMSO until fully dissolved. Therefore, WO concentrations are reported as µL/mL (v/v) based on the final DMSO stock solution.

2.3. MTT Cytotoxicity Assay

Cell viability was assessed using the 3-(4,5-Dimethylthiazol-2-yl)-2,5-Diphenyltetrazolium Bromide (MTT) assay. T98-G cells were seeded in 96-well plates at a density of 4,000 cells/well and treated with varying concentrations of wormwood total extract (WO; 2–20 µL/mL; v/v, defined as µL of WO stock extract per mL of culture medium) or temozolomide (TMZ; 1–1000 µM) for 24 and 48 hours. After treatment, 4 µL of MTT reagent (0.1 mM Sigma-Aldrich, M2128) was added to each well and incubated for 4 hours. Formazan crystals were dissolved in DMSO and absorbance was measured at 570 nm. IC_{50} values were calculated using GraphPad Prism 9.0.

2.4. Annexin V-FITC/PI Apoptosis Assay

Apoptosis was analyzed using the Annexin V-FITC/PI kit (BD Biosciences, 556547). Cells treated with IC_{50} concentrations of WO, TMZ, or their combination were stained with Annexin V-FITC and PI. Stained samples were analyzed via flow cytometry (BD Accuri™ C6 Plus) and data were processed using FlowJo software.

2.5. Monodansylcadaverine (MDC) Staining for Autophagy

Autophagic vacuoles were detected via MDC staining. Cells were grown on glass coverslips in 24-well plates until reaching 50% confluency. After 48 hours of treatment, cells were incubated with 0.05 mM MDC in serum- and antibiotic-free medium at 37°C for 7 minutes. Stained cells were rinsed with PBS and visualized using a fluorescence microscope (Olympus BX43) with a DAPI filter.

2.6. JC-1 Mitochondrial Membrane Potential Assay

Mitochondrial membrane potential was evaluated using JC-1 dye (Cayman Chemical, 10009172). Cells treated with IC_{50} concentrations were stained with JC-1 for 7 minutes and fluorescence images were captured using an Olympus IX73 microscope. The red-to-green fluorescence ratio was quantified using ImageJ software.

2.7. Wound Healing Assay

Cell migration was evaluated using a wound healing (scratch) assay. Confluent cell monolayers were scratched with a sterile pipette tip and subsequently treated with IC_{50} concentrations of WO, TMZ, or their combination. Wound closure was monitored at 0, 12, 24, 36, and 48 hours under an inverted microscope (Zeiss Axio Vert.A1). The migration rate was quantified by calculating the percentage of gap closure using ImageJ software.

2.8. Immunofluorescence Staining

Cells treated with IC_{50} concentrations were fixed, permeabilized, and blocked using 5% bovine serum albumin (BSA; Sigma-Aldrich, A7906). Primary antibodies against endothelial nitric oxide synthase (eNOS) (Abcam, ab66127), inducible nitric oxide synthase (iNOS) (Abcam, ab15323), and LC3 (Abcam, ab58610) were applied, followed by FITC-conjugated secondary antibodies (Abcam, ab6717). Nuclei were counterstained with DAPI (Sigma-Aldrich, D9542). Fluorescence images were captured using an Olympus BX53 microscope and processed with Adobe Photoshop CC.

2.9. Western Blotting

2.9.1. Protein extraction and quantification

Cells grown in 6-well plates were treated with IC_{50} doses and incubated for 48 h. After removing the medium and washing with PBS, 300 µL M-PER reagent (Thermo Fisher) containing 3 µL protease inhibitor cocktail was added per well. Lysates were centrifuged at 14,000 × g for 15 min at 4°C and supernatants were collected (20 µL aliquots) for analysis. Protein concentration was determined using the Pierce™ BCA Protein Assay Kit (Thermo Scientific, Cat. No. 23225) by mixing 10 µL of each sample with 200 µL of BCA working solution, incubating at 37°C for 30 min, and measuring absorbance with a Nanodrop spectrophotometer**.**

2.9.2. Gel Electrophoresis and blotting

SDS-PAGE was performed with stacking (4–7% acrylamide) and resolving (7–17%) gels. Protein samples (0.9 mg/mL) were mixed 1:1 with Laemmli buffer containing β-mercaptoethanol and boiled at 95°C for 5 minutes. Samples were loaded onto gels and run at 90 V for 120–150 minutes using the Mini-PROTEAN System (Bio-Rad).

Proteins were transferred to PVDF membranes (Bio-Rad, Cat. No. 1620177) at 30 V for 14 hours at 4°C. Membranes were blocked in TBS-T with 5% skimmed milk for 30 minutes and incubated with primary antibodies (eNOS, iNOS, LC3-I/II, β-actin) at a 1:1000 dilution overnight at 4°C. After washing, membranes were incubated with HRP-conjugated secondary antibodies (1:1000 dilution) for 1 hour. Bands were visualized by using diaminobenzidine (DAB) solution and quantified by using ImageJ software.

2.10. Statistical Analysis

Results are expressed as mean ± standard deviation (SD). Statistical analyses were conducted using one-way ANOVA followed by Dunnett's post-hoc test in GraphPad Prism 9.3.1. A p-value<0.05 was considered statistically significant.

3. Results

3.1. MTT Assay

MTT assay results revealed that WO significantly reduced T98-G cell viability in a dose- and time-dependent manner, with pronounced cytotoxicity observed at 48 and 72 hours. Based on these findings, 24 hours was selected as the optimal exposure time and the IC_{50} value of WO was calculated as 6.91 µl/ml (Fig. 1A). TMZ demonstrated an IC_{50} value of 391.4 µM for 24-hour exposure (Fig. 1B).

3.2. Annexin V/PI Flow Cytometry Analysis

Flow cytometric Annexin V/PI analysis revealed treatment-dependent apoptotic shifts in T98-G cells (Fig. 2). The control group consisted predominantly of viable cells (91.8%) with minimal early (5.1%) or late apoptosis (1.2%). WO IC_{50} increased early and late apoptosis to 18.9% and 24.3%, respectively, reducing viability to 54.7%. TMZ IC_{50} induced moderate apoptosis with 33.7% early and 5.3% late apoptotic cells (viable: 60.5%). The combined treatment produced the strongest effect, elevating early apoptosis to 24.6% and late apoptosis to 40.5% with viability declining to 31.9%. Collectively, these findings indicate that the combined treatment produces the most pronounced apoptotic response in T98-G cells.

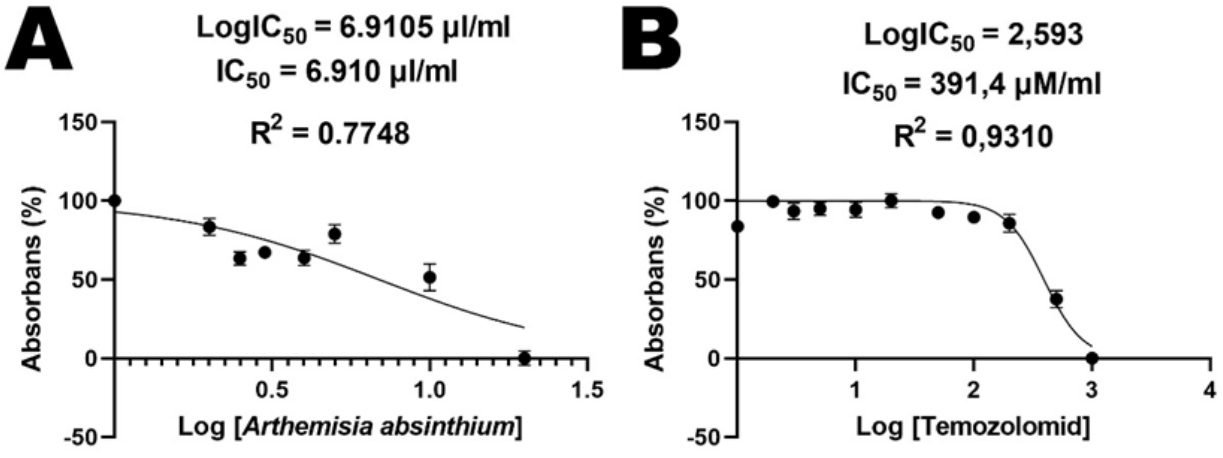

Figure 1. The cytotoxic effects of WO (A) and TMZ (B) applied at various doses on T98-G cells.

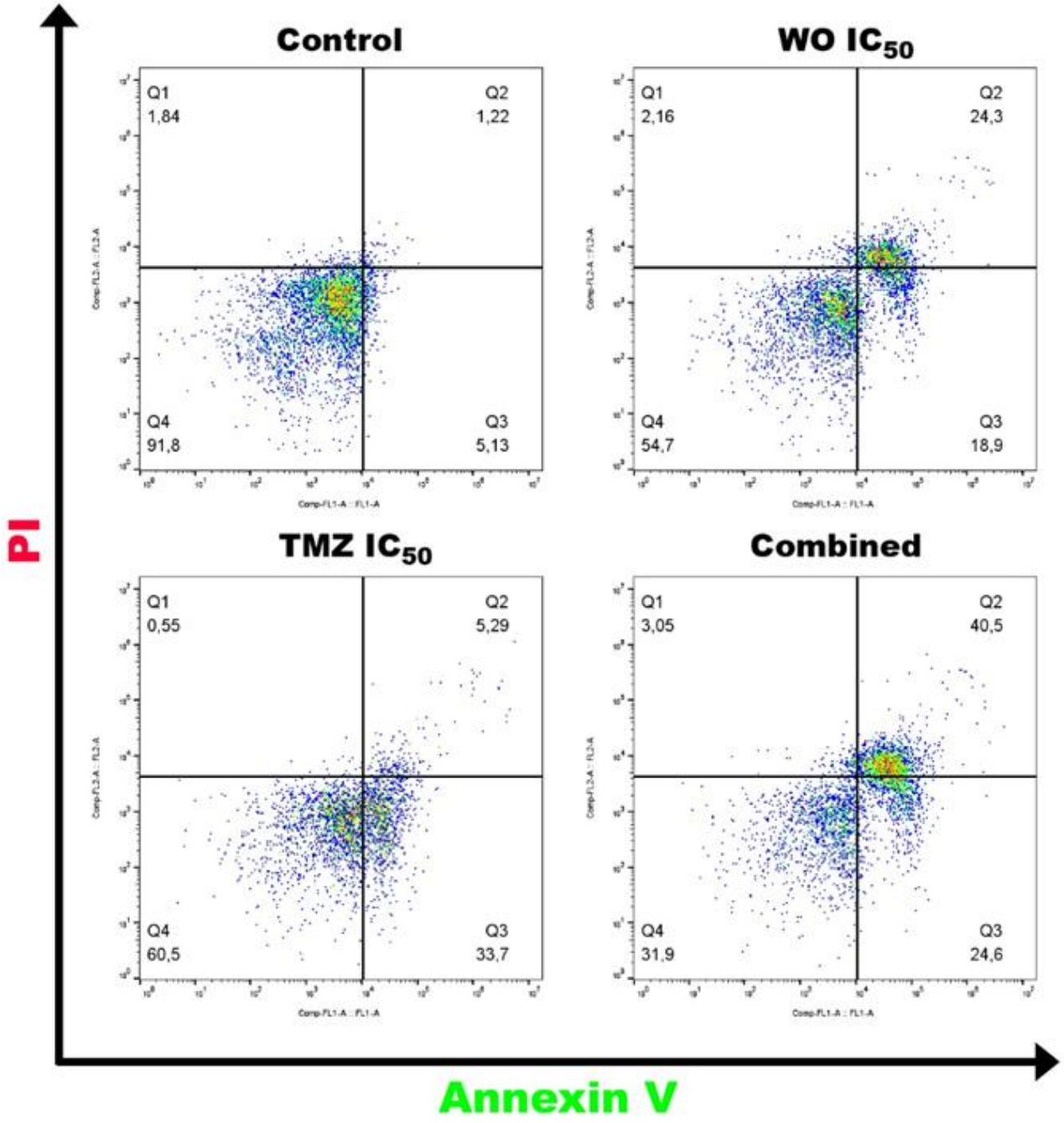

Figure 2. Annexin V/PI flow cytometry results for T98-G cells.

3.3. MDC Imaging

Autophagic vacuoles were detected in the cytoplasm, particularly in the perinuclear region, across both control and treatment groups (Fig. 3). A dose-dependent increase in vacuole number and noticeable variations in intracellular localization were observed in the treated cells compared to the controls. In the WO IC_{50} and IC_{75} groups, vacuoles were more prominent and predominantly concentrated around the nucleus. In the TMZ IC_{25} and IC_{50} groups, the vacuoles appeared enlarged and were distributed both perinuclearly and throughout the cytoplasm. The combination treatment displayed a pattern similar to TMZ IC_{25} and IC_{50} with an evident enhancement of TMZ-induced effects.

3.4. JC-1 Staining

Upon fluorescence microscopy analysis of mitochondrial membrane potential across the different treatment groups (Fig. 4), the control condition exhibited a strong red fluorescence signal, indicative of preserved mitochondrial integrity and normal membrane polarization. As anticipated, the positive control CCCP induced a prominent increase in green fluorescence, thereby confirming a complete dissipation of mitochondrial membrane potential. In cells treated with the IC_{50} concentration of WO, the simultaneous presence of red and green signals reflected partial depolarization accompanied by structural mitochondrial alterations. Treatment with TMZ at its IC_{50} concentration largely maintained mitochondrial membrane potential; however, the mitochondria displayed a more punctate and fragmented morphology. The most pronounced alterations were observed in the combined treatment group, which demonstrated a substantial reduction in

membrane potential together with marked mitochondrial fragmentation. Collectively, these findings suggest that concomitant administration of WO and TMZ elicits a more profound—and potentially enhanced—disruption of mitochondrial function compared with either of them.

3.5. Cell Migration Assay

Cell migration was significantly suppressed in all treatment groups compared to the control (Fig. 5). While the control group exhibited almost complete wound closure by 48 hours, WO IC_{50} caused the most pronounced inhibition of migration with less than 20% closure observed beyond 24 hours. TMZ IC_{50} and the combination treatment showed moderate inhibition, resulting in approximately 40–45% wound closure at 48 hours. These results suggest that WO is the most potent inhibitor of cell migration among the tested conditions.

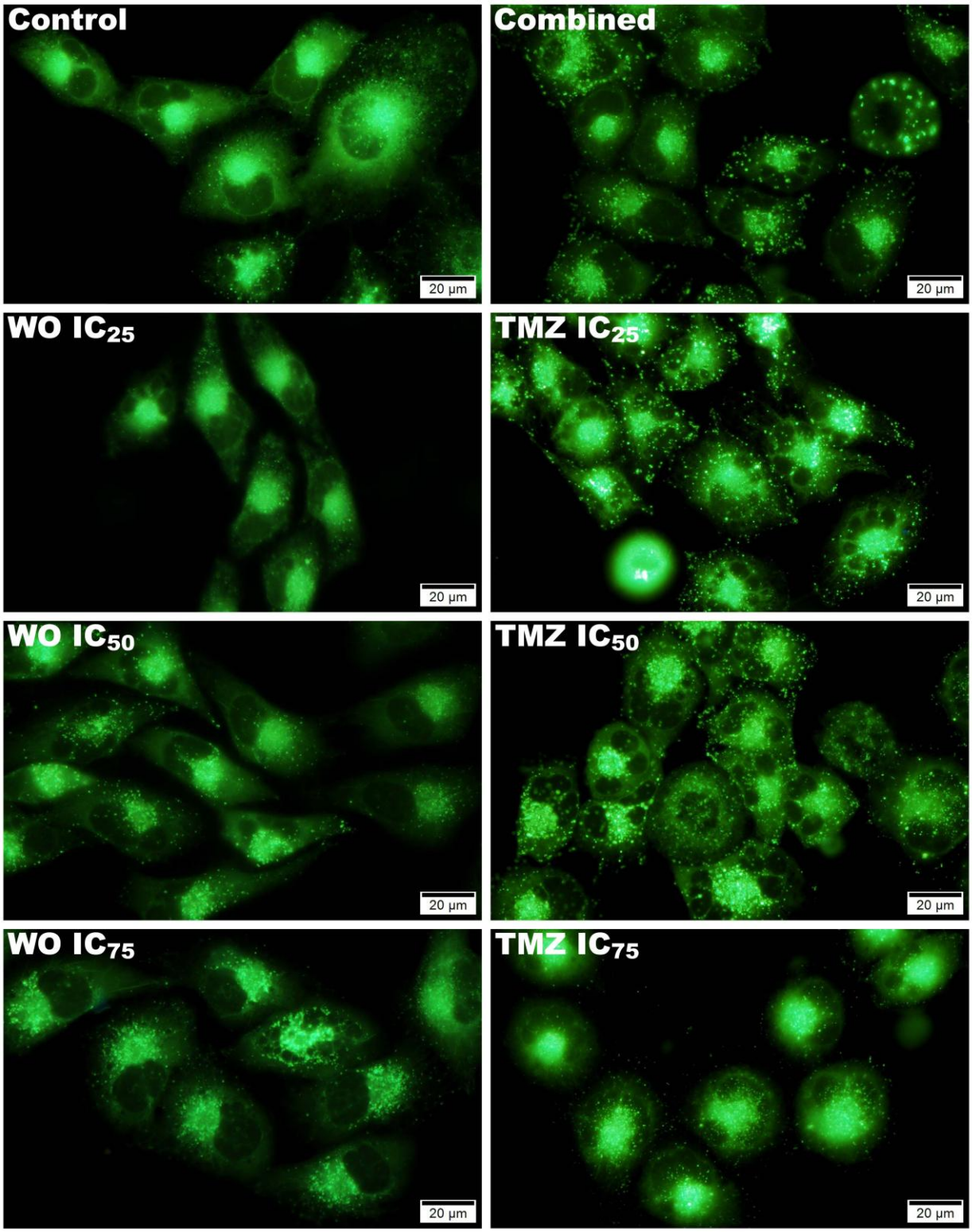

Figure 3. The changes induced by WO, Temozolomide (TMZ), and their combination treatments on vesicles were analyzed using MDC staining (Scale bar: 20 µm).

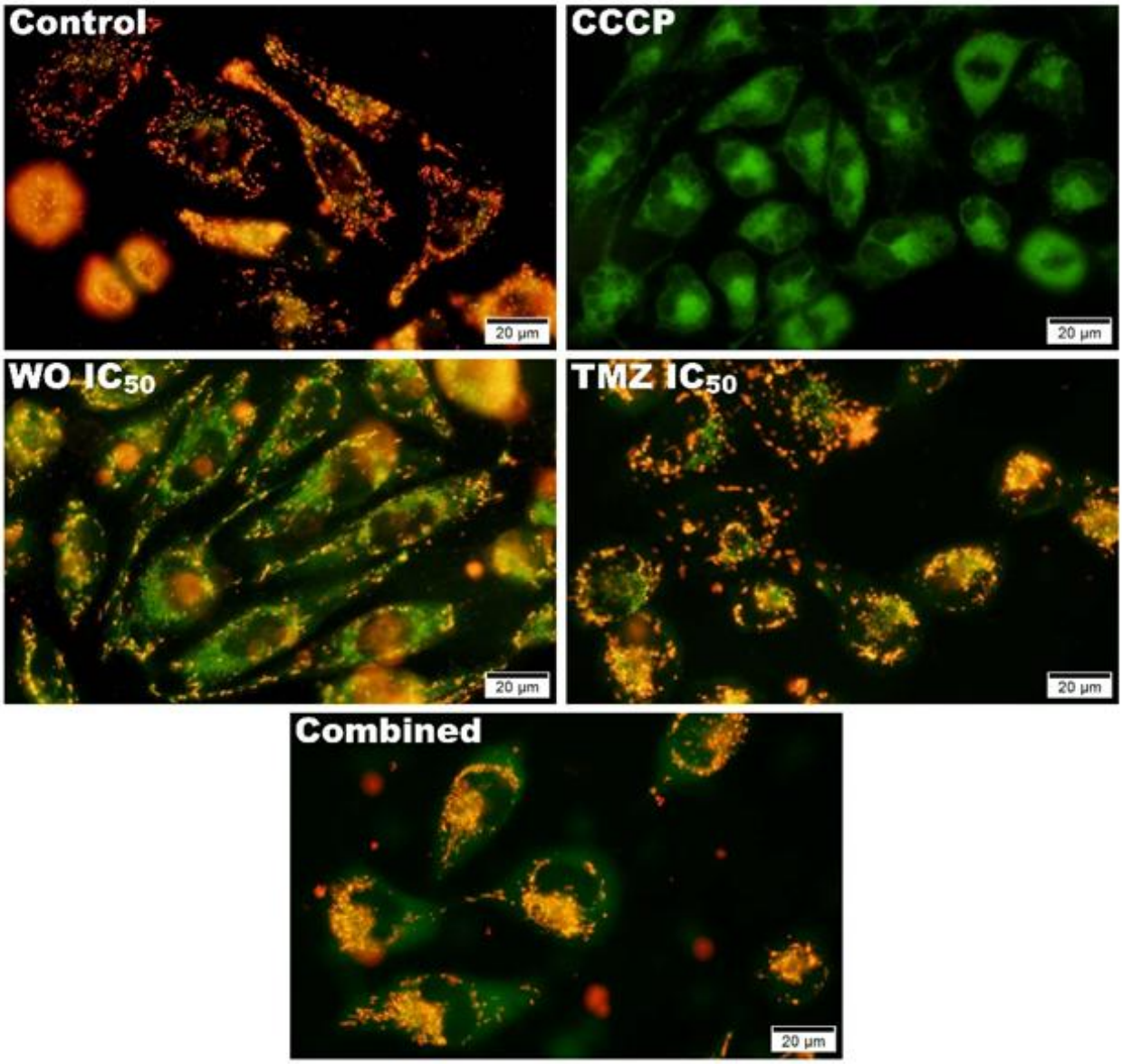

Figure 4. JC-1 staining groups for T98-G cells. (-) Control: untreated cells in culture medium; (+) Control: CCCP-treated cells disrupting mitochondrial membrane potential. Scale bar: 20 µm.

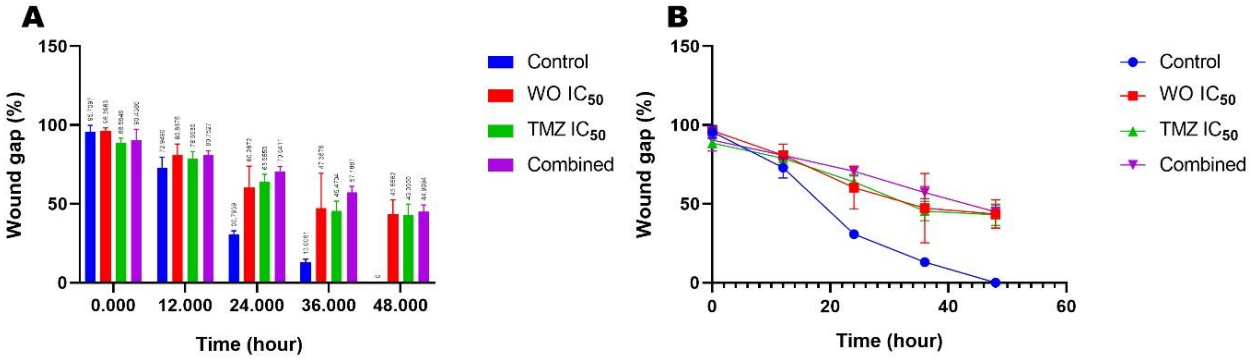

Figure 5. WO inhibits migration of T98-G glioblastoma cells. (A) Normalized wound closure percentages at different time points following treatment with WO IC_{50}, TMZ IC_{50}, or their combination. (B) Time-course analysis of wound closure expressed as % of control. Data were normalized to 0 h (100%) and are presented as mean ± SD (n ≥ 3).

3.6. Immunofluorescence Imaging

3.6.1. eNOS Staining

The eNOS expression in T98-G cells was evaluated using immunofluorescence staining (Fig. 6). Control cells exhibited a uniform cytoplasmic distribution of eNOS (green fluorescence) with distinct perinuclear localization (red arrows). Treatment with WO at its IC_{50} concentration increased eNOS signal intensity compared with the control and preserved a predominantly cytoplasmic/perinuclear

pattern. TMZ IC_{50} and the combined treatment did not show a clear increase in eNOS fluorescence relative to the control; however, both conditions showed a more diffuse and less organized staining pattern in some cells. Overall, these observations are consistent with the quantitative CTCF measurements shown in Fig. 6.

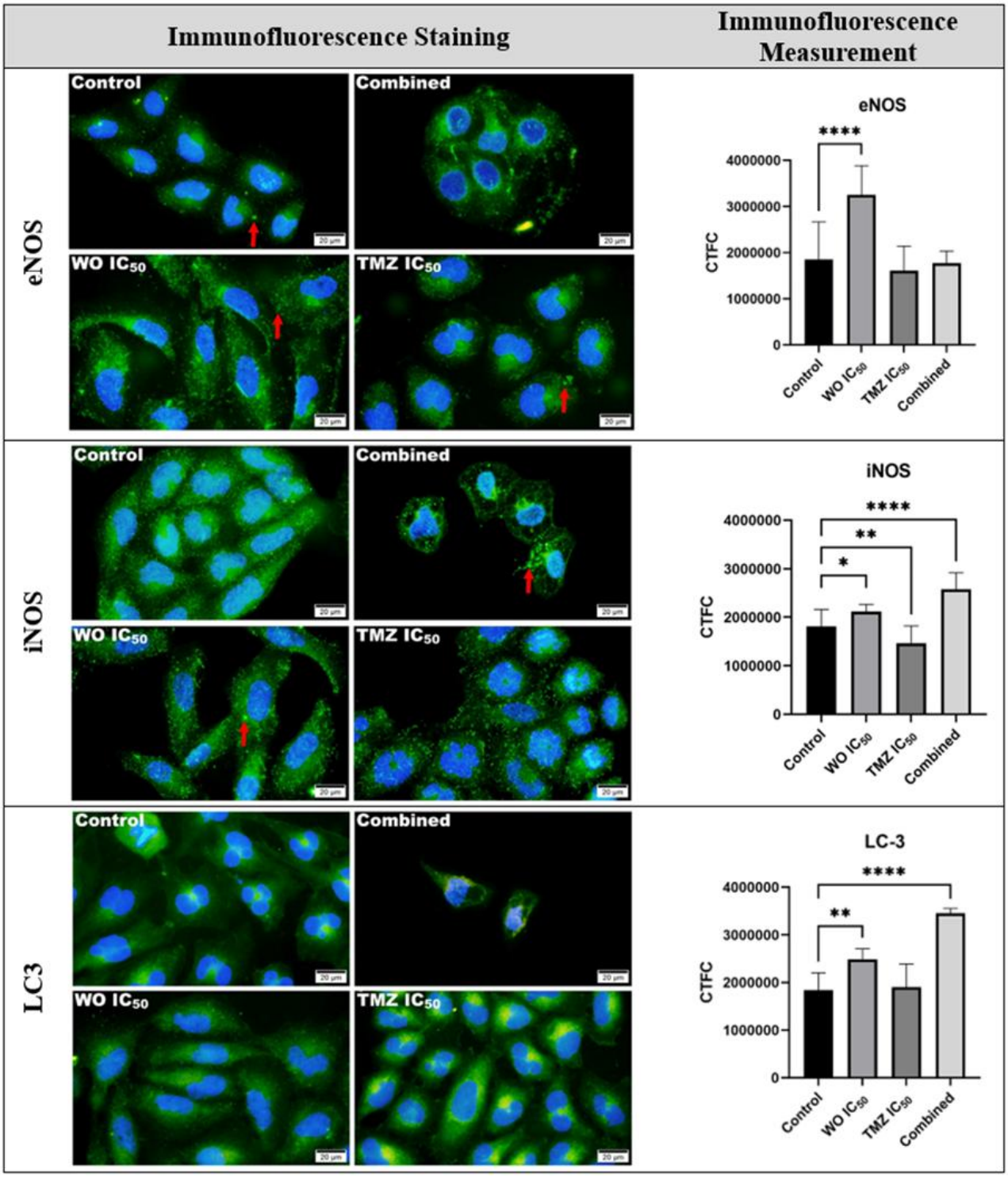

Figure 6. In the top-left panel, eNOS, iNOS, and LC3 immunofluorescence staining images of T98-G cells are shown (arrow indicates vesicles) (scale bar: 20 μm). In the top-right panel, pixel intensity graphs of eNOS, iNOS, and LC3 immunocytochemical staining are presented (CTCF: corrected total cell fluorescence).

3.6.2. iNOS Staining

The images comparatively illustrate the effects of different treatment conditions on cellular morphology and protein distribution (Fig. 6). In the control group, cells exhibit a regular morphology with a homogeneous cytoplasmic distribution of the targeted protein. In contrast, treatment with WO IC_{50} and TMZ IC_{50} results in a more granular fluorescence pattern accompanied by localized cytoplasmic accumulation and noticeable morphological alterations. Notably, the combined treatment group displays a marked reduction in cell number, increased cytoplasmic signal aggregation, and pronounced morphological deterioration, suggesting that the combination induces stronger cellular stress and a

potentially higher cytotoxic effect compared to the single-agent treatments.

3.6.3. LC3 Staining

Immunofluorescence analysis was performed using an antibody recognizing total LC3 and therefore does not distinguish between LC3-I and LC3-II. Accordingly, LC3 puncta formation was evaluated as an indicator of autophagosome accumulation. LC3 immunofluorescence staining revealed distinct alterations in autophagic activity in T98-G cells under different treatment conditions (Fig. 6). In the control group, LC3 displayed a diffuse cytoplasmic distribution with minimal puncta formation indicating basal autophagy levels. Treatment with WO IC_{50} or TMZ IC_{50} resulted in an evident increase in LC3 puncta, accompanied by a more granular fluorescence pattern, suggesting enhanced autophagosome formation. The most pronounced effect was observed in the combined treatment group where a marked reduction in cell number was accompanied by strong LC3 accumulation and dense puncta formation. These findings indicate that the combined treatment induces a more robust autophagic response in T98-G cells compared with either agent alone.

3.6.4. Immunofluorescence Measurements

In T98-G cells, eNOS expression (CTFC) showed significant variation among treatment groups (Fig. 6). WO IC_{50} markedly increased eNOS levels compared with the control ($p<0.0001$). In contrast, TMZ IC_{50} and the combined treatment did not produce significant differences relative to the control ($p>0.05$). These findings indicate that WO IC_{50} selectively elevates eNOS expression in T98-G cells, whereas TMZ IC_{50} alone or in combination does not.

Quantitative fluorescence analysis revealed significant treatment-dependent alterations in iNOS expression in T98-G cells (Fig. 6). Compared with the control group, WO IC_{50} treatment induced a marked increase in iNOS fluorescence intensity (**** $p<0.0001$), whereas TMZ IC_{50} treatment resulted in a moderate but significant elevation (* $p<0.05$). Additionally, iNOS levels were significantly higher in the TMZ IC_{50} group compared with the WO IC_{50} group (** $p<0.01$) indicating differential regulatory effects between the two treatments. The combined treatment produced the highest iNOS fluorescence intensity among all groups, showing a highly significant increase relative to the control (**** $p<0.0001$). These data demonstrate that combined exposure triggers a more robust upregulation of iNOS in T98-G cells compared with single-agent treatments.

In T98-G cells, LC3 expression (CTFC) significantly increased following WO IC_{50} treatment compared with the control ($p<0.01$). Moreover, the combined treatment produced the highest LC3 level, showing a highly significant increase relative to all other groups ($p<0.0001$). TMZ IC_{50} alone did not differ significantly from the control ($p>0.05$). These findings indicate that WO IC_{50} enhances LC3 expression and this effect is further amplified under the combined treatment (Fig. 6).

3.7. Western Blotting Analysis

Western blotting was performed to evaluate the expression of eNOS, iNOS, and LC3-II with β-actin serving as the loading control (Fig. 7). Densitometric analysis revealed that eNOS expression increased in the WO IC_{50} group compared to the control, peaking at WO IC_{50}, whereas TMZ IC_{50} treatment significantly reduced eNOS levels. The combination group (WO + TMZ) showed intermediate expression, higher than TMZ but slightly below control levels.

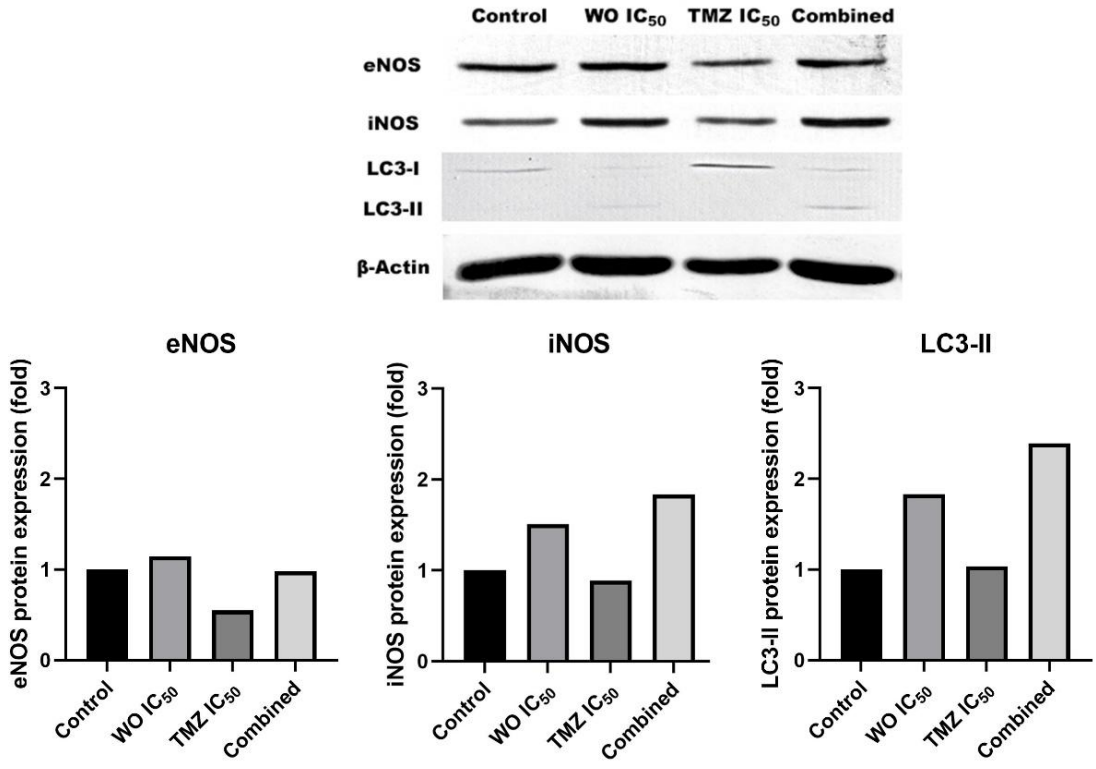

Figure 7. Western blotting analysis of eNOS, iNOS, and LC3-II protein expression.

For iNOS, WO IC_{50} treatment resulted in a notable increase in expression relative to the control, while TMZ IC_{50} caused a decrease. The combination group displayed the highest iNOS expression among all groups, suggesting a counteractive effect of WO on TMZ-mediated suppression.

LC3-II expression, indicative of autophagy, increased in a dose-dependent manner with WO treatment. Although TMZ IC_{50} also enhanced LC3-II levels compared to the control, the combination treatment induced the strongest LC3-II signal indicating potentiated autophagic activity when WO and TMZ were co-administered.

4. Discussion

This study provides novel evidence for the anticancer potential of *A. absinthium (WO)* in glioblastoma as it clearly demonstrates its cytotoxic, pro-apoptotic, autophagy-inducing, and anti-migratory effects in T98-G cells both alone and in combination with temozolomide (TMZ). WO significantly reduced cell viability in a dose- and time-dependent manner with notable cytotoxicity observed at 48 and 72 hours and an IC_{50} value of 6.91 µl/ml at 24 hours. These results align with the previous studies reporting that *A. absinthium* extracts suppress proliferation and promote cell death in several cancer models through oxidative stress–related and mitochondrial pathways (Singh & Lai, 2004; Mughees et al., 2020; He et al., 2023; Tsamesidis et al., 2024). The IC_{50} value obtained for TMZ (391.4 µM) is consistent with the known chemoresistant phenotype of T98-G cells, emphasizing the need for adjunct treatments that can enhance TMZ efficacy.

Annexin V-FITC/PI analyses confirmed that WO strongly induces apoptosis by increasing both early and late apoptotic populations. Notably, the WO + TMZ combination produced a substantial elevation in late apoptosis compared with either treatment alone indicating an enhanced combined effect. Because we did not perform a formal synergy analysis (e.g., combination index), the combined effects are described conservatively as "enhanced" rather than synergistic. This enhanced effect may reflect the ability of WO to sensitize glioblastoma cells to TMZ by intensifying mitochondrial destabilization or oxidative damage. Similar observations have been reported in other cancer models where constituents of *A. absinthium*, such as sesquiterpenes and flavonoids, activate caspase-mediated apoptosis while sparing normal cells (Wei et al., 2019).

Consistent with this apoptotic shift, JC-1 staining revealed that WO promotes mitochondrial membrane depolarization in a dose-dependent manner. The loss of mitochondrial membrane potential ($\Delta\Psi m$) observed with JC-1, indicated by a decrease in red fluorescence and an increase in green fluorescence in the WO and WO+TMZ groups, points to mitochondrial dysfunction and cell death. TMZ also induced mitochondrial dysfunction but the combined treatment resulted in the most prominent loss of membrane potential. This finding supports the central role of mitochondrial perturbation in WO-mediated apoptosis and suggests that WO may enhance TMZ-induced cytotoxicity by targeting mitochondrial integrity. The findings of our study regarding WO-induced mitochondrial depolarization are consistent with previous reports on *A. absinthium* extracts. Methanolic extract of *A. absinthium* (MEAA) significantly reduced HCT-116 colorectal cancer cell viability, induced apoptosis, and caused a marked disruption of mitochondrial membrane potential (Koyuncu, 2018; Nazeri et al., 2020). Considering previous studies and our findings, it is suggested that the mitochondrial pathway may be the primary mechanism underlying apoptosis induced by *A. absinthium.*

WO also exerted a strong inhibitory effect on cell migration, surpassing the anti-migratory activity of TMZ. Given the highly infiltrative nature of glioblastoma, the suppression of cell migration by WO is noteworthy. Although studies on Artemisia species and cancer cell migration are limited, some reports indicate that Artemisia extracts can modulate metastasis-related pathways, including MMP-2/MMP-9 activity and epithelial–mesenchymal transition, which may explain the reduced migratory capacity observed in this study (He et al., 2023).

In our study, treatment-dependent changes in eNOS and iNOS levels were observed. This is an interesting and rarely investigated finding in the literature as most previous studies have focused primarily on ROS, mitochondria, and apoptosis with little attention given to NO/NOS signaling or nitrogen radicals. The present findings further highlight a modulatory effect of WO on nitric oxide synthase (NOS) signaling. Immunofluorescence and Western blot analyses showed that WO increased eNOS expression at moderate doses, whereas TMZ reduced eNOS levels. The combination treatment yielded intermediate expression indicating a partial counteraction of TMZ-induced suppression. For iNOS, WO increased expression and cytoplasmic vesicle-like localization in a dose-dependent manner, while TMZ markedly downregulated iNOS. Interestingly, the combination treatment exhibited the highest iNOS expression, suggesting that WO may reverse the inhibitory effects of TMZ on inflammatory NOS signaling. The prominent perinuclear accumulation of iNOS-containing vesicles may reflect heightened cellular stress responses, although further studies are necessary to determine their exact functional role.

Autophagic responses were also significantly influenced by WO. LC3 immunofluorescence and LC3-II Western blot data indicated that WO induces autophagy in a dose-dependent manner. TMZ similarly increased LC3-II levels at its IC_{50} concentration, yet the combined treatment triggered the strongest autophagic activation. These findings suggest that WO may potentiate TMZ-induced autophagy. While autophagy can be either cytoprotective or cytotoxic, the concurrent increase in apoptosis observed here indicates that WO-associated autophagy likely contributes to cell death rather than survival in T98-G cells. Although studies on *A. absinthium* derivatives are limited in the literature, umbelliprenin isolated from *A. absinthium* L. has been reported to induce autophagy in BxPC3 and PANC-1 pancreatic cancer cell lines (Wang et al., 2023). We observed an increase in autophagy; however, determining whether this increase contributes to cell death or instead promotes survival and adaptation requires further testing using autophagy inhibitors or genetic manipulation approaches.

Overall, the results of this study demonstrate that

WO exerts multifaceted antitumor effects in glioblastoma, targeting apoptosis, mitochondrial function, autophagy, cell migration, and NOS responses. The enhanced apoptotic and autophagic responses observed in the WO + TMZ group highlight the potential of WO as an adjuvant therapeutic candidate capable of overcoming TMZ resistance. Given the scarcity of studies evaluating *A. absinthium* in glioblastoma, the present findings provide a valuable foundation for further mechanistic research and preclinical evaluation.

This study was conducted *in vitro* using a single glioblastoma cell line (T98-G); given the complex heterogeneity and microenvironment of glioblastoma, *in vivo* models (e.g., tumor-bearing mouse models) will be essential for future validation. The chemical composition of the WO extract (flavonoids, terpenoids, phenolics, etc.) was not characterized in this work, although previous studies suggest that specific fractions of *A. absinthium* may contribute significantly to cytotoxicity. Phytochemical profiling (LC-MS/MS, fractionation) and identification of active components would be more appropriately addressed in a separate future study.

Moreover, although our findings on NO/NOS signaling are promising, the functional role of these pathways—whether pro-apoptotic or adaptive stress responses—remains unclear. Future studies should include NOS inhibition/modulation, ROS/RNS quantification, and additional mechanistic analyses to clarify their contribution.

One limitation of this study is that the Western blot analyses could not be performed with three independent replicates, preventing the acquisition of statistically robust quantitative data.

5. Conclusion

In conclusion, this study demonstrates that *A. absinthium* exhibits strong cytotoxic, pro-apoptotic, autophagy-inducing, and anti-migratory activities in T98-G glioblastoma cells and enhances the cytotoxic efficacy of TMZ when used in combination. These results suggest that WO or its bioactive constituents may represent promising adjuvant therapeutic candidates for improving treatment outcomes in TMZ-resistant glioblastoma. However, comprehensive phytochemical characterization, *in vivo* validation, and deeper molecular analyses are required before clinical translation can be considered. Overall, observed multi-pathway effects — including mitochondrial dysfunction, ROS/NOS modulation, apoptosis, autophagy, and migration inhibition — indicate that *A. absinthium* has substantial potential as a novel complementary strategy in glioblastoma therapy.

Acknowledgment: The authors thank the Scientific Research Projects Committee of Manisa Celal Bayar University for supporting this work (Project No. 2022-025).

Ethics committee approval: Ethics committee approval is not required for this study.

Conflict of interest: The authors declare that there is no conflict of interest.

Author Contributions: Conception – B.G., F.Ç.; Design – B.G., F.Ç.; Supervision – B.G.; Fund – B.G.; Materials – B.T., B.G.; Data Collection or Processing – F.Ç.; Analysis Interpretation – B.T., F.Ç.; Literature Review – B.T.; Writing – B.T.; Critical Review – B.T.

References

Batash, R., Asna, N., Schaffer, P., Francis, N., & Schaffer, M. (2017). Glioblastoma multiforme, diagnosis and treatment; recent literature review. *Current Medicinal Chemistry*, *24*(27), 3002–3009. https://doi.org/10.2174/0929867324666170516123206

Batiha, G.E., Olatunde, A., El-Mleeh, A., Hetta, H.F., Al-Rejaie, S., Alghamdi, S., Zahoor, M., Magdy Beshbishy, A., Murata, T., Zaragoza-Bastida, A., & Rivero-Perez, N. (2020). Bioactive compounds, pharmacological actions, and pharmacokinetics of wormwood (*Artemisia absinthium*). *Antibiotics (Basel, Switzerland)*, *9*(6), 353. https://doi.org/10.3390/antibiotics9060353

Bora, K.S., & Sharma, A. (2010). Neuroprotective effect of *Artemisia absinthium* L. on focal ischemia and reperfusion-induced cerebral injury. *Journal of Ethnopharmacology*, *129*(3), 403–409. https://doi.org/10.1016/j.jep.2010.04.030

Caner, A., Döşkaya, M., Değirmenci, A., Can, H., Baykan, S., Uner, A., Başdemir, G., Zeybek, U., & Gürüz, Y. (2008). Comparison of the effects of *Artemisia vulgaris* and *Artemisia absinthium* growing in western Anatolia against trichinellosis (Trichinella spiralis) in rats. *Experimental Parasitology*, *119*(1), 173–179. https://doi.org/10.1016/j.exppara.2008.01.012

Dehelean, C.A., Marcovici, I., Soica, C., Mioc, M., Coricovac, D., Iurciuc, S., Cretu, O.M., & Pinzaru, I. (2021). Plant-derived anticancer compounds as new perspectives in drug discovery and alternative therapy. *Molecules (Basel, Switzerland)*, *26*(4), 1109. https://doi.org/10.3390/molecules26041109

He, M., Yasin, K., Yu, S., Li, J., & Xia, L. (2023). Total Flavonoids in *Artemisia absinthium* L. and evaluation of ıts anticancer activity. *International Journal of Molecular Sciences*, *24*(22), 16348. https://doi.org/10.3390/ijms242216348

Kashyap, D., Tuli, H.S., Yerer, M.B., Sharma, A., Sak, K., Srivastava, S., Pandey, A., Garg, V.K., Sethi, G., & Bishayee, A. (2021). Natural product-based nanoformulations for cancer therapy: Opportunities and challenges. *Seminars in Cancer Biology*, *69*, 5–23. https://doi.org/10.1016/j.semcancer.2019.08.014

Koyuncu I. (2018). Evaluation of anticancer, antioxidant activity and phenolic compounds of *Artemisia absinthium* L. Extract. *Cellular and Molecular Biology (Noisy-le-Grand, France)*, *64*(3), 25–34. https://doi.org/10.14715/cmb/2018.64.3.5

Mahmoudi, M., Ebrahimzadeh, M.A., Ansaroudi, F., Nabavi, S.F., & Nabavi, S.M. (2009). Antidepressant and antioxidant activities of *Artemisia absinthium* L. at flowering stage. *African Journal of Biotechnology*, *8*(24), 7170–7175. https://doi.org/10.5897/AJB09.753

Mughees, M., Wajid, S., & Samim, M. (2020). Cytotoxic potential of *Artemisia absinthium* extract loaded polymeric nanoparticles against breast cancer cells: Insight into the protein targets. *International Journal of Pharmaceutics*, *586*, 119583. https://doi.org/10.1016/j.ijpharm.2020.119583

Nazeri, M., Mirzaie-Asl, A., Saidijam, M., & Moradi, M. (2020). Methanolic extract of *Artemisia absinthium* prompts apoptosis, enhancing expression of Bax/Bcl-2 ratio, cell cycle arrest, caspase-3 activation and mitochondrial membrane potential destruction in human colorectal cancer HCT-116 cells. *Molecular Biology Reports*, *47*(11), 8831–8840. https://doi.org/10.1007/s11033-020-05933-2

Park, J.H., & Lee, H.K. (2022). Current understanding of hypoxia in glioblastoma multiforme and its response to immunotherapy. *Cancers*, *14*(5), 1176. https://doi.org/10.3390/cancers14051176

Parpura, V., Heneka, M.T., Montana, V., Oliet, S.H., Schousboe, A., Haydon, P.G., Stout, R.F., Jr, Spray, D.C., Reichenbach, A., Pannicke, T., Pekny, M., Pekna, M., Zorec, R., & Verkhratsky, A. (2012). Glial cells in (patho) physiology. *Journal of Neurochemistry*, *121*(1), 4–27. https://doi.org/10.1111/j.1471-4159.2012.07664.x

Pfeffer, C.M., & Singh, A.T.K. (2018). Apoptosis: A target for anticancer therapy. *International Journal of Molecular Sciences*, *19*(2), 448. https://doi.org/10.3390/ijms19020448

Ramazani, A., Sardari, S., Zakeri, S., & Vaziri, B. (2010). *In vitro* antiplasmodial and phytochemical study of five *Artemisia* species from Iran and *in vivo* activity of two species. *Parasitology Research*, *107*(3), 593–599. https://doi.org/10.1007/s00436-010-1900-4

Singh, N.P., & Lai, H.C. (2004). Artemisinin induces apoptosis in human cancer cells. *Anticancer Research*, *24*(4), 2277–2280.

Tsamesidis, I., Papadimitriou-Tsantarliotou, A., Christodoulou, A., Amanatidou, D., Avgeros, C., Stalika, E., Bousnaki, M., Michailidou, G.,

Beketova, A., Eleftheriou, P., Bikiaris, D.N., Vizirianakis, I.S., & Kontonasaki, E. (2024). Investigating the cytotoxic effects of *Artemisia absinthium* extract on oral carcinoma cell line. *Biomedicines*, *12*(12), 2674. https://doi.org/10.3390/biomedicines12122674

Wang, H., Liu, Y., Wang, Y., Xu, T., Xia, G., & Huang, X. (2023). Umbelliprenin induces autophagy and apoptosis while inhibits cancer cell stemness in pancreatic cancer cells. *Cancer Medicine*, *12*(14), 15277–15288. https://doi.org/10.1002/cam4.6170

Wei, X., Xia, L., Ziyayiding, D., Chen, Q., Liu, R., Xu, X., & Li, J. (2019). The extracts of *Artemisia absinthium* L. suppress the growth of hepatocellular carcinoma cells through induction of apoptosis via endoplasmic reticulum stress and mitochondrial-dependent pathway. *Molecules*, *24*(5), 913. https://doi.org/10.3390/molecules24050913